



HAL
open science

A poromechanical model for coal seams saturated with binary mixtures of CH₄ and CO₂

Saeid Nikoosokhan, Matthieu Vandamme, Patrick Dangla

► **To cite this version:**

Saeid Nikoosokhan, Matthieu Vandamme, Patrick Dangla. A poromechanical model for coal seams saturated with binary mixtures of CH₄ and CO₂. *Journal of the Mechanics and Physics of Solids*, 2014, 71, pp.97-111. 10.1016/j.jmps.2014.07.002 . hal-01085940

HAL Id: hal-01085940

<https://enpc.hal.science/hal-01085940>

Submitted on 4 Feb 2015

HAL is a multi-disciplinary open access archive for the deposit and dissemination of scientific research documents, whether they are published or not. The documents may come from teaching and research institutions in France or abroad, or from public or private research centers.

L'archive ouverte pluridisciplinaire **HAL**, est destinée au dépôt et à la diffusion de documents scientifiques de niveau recherche, publiés ou non, émanant des établissements d'enseignement et de recherche français ou étrangers, des laboratoires publics ou privés.

A poromechanical model for coal seams saturated with binary mixtures of CH₄ and CO₂

Saeid Nikoosokhan^a, Matthieu Vandamme^a, Patrick Dangla^{b,*}

^a *Université Paris-Est, Laboratoire Navier (UMR 8205), CNRS, ENPC, IFSTTAR, F-77455 Marne-la-Vallée, France*

^b *Université Paris-Est, Laboratoire Navier (UMR 8205), CNRS, ENPC, IFSTTAR, F-77420 Marne-la-Vallée, France*

Abstract

Underground coal bed reservoirs naturally contain methane which can be produced. In parallel of the production of this methane, carbon dioxide can be injected, either to enhance the production of methane, or to have this carbon dioxide stored over geological periods of time. As a prerequisite to any simulation of an Enhanced Coal Bed Methane recovery process (ECBM), we need state equations to model the behavior of the seam when cleats are saturated with a miscible mixture of CH₄ and CO₂. This paper presents a poromechanical model of coal seams exposed to such binary mixtures filling both the cleats in the seam and the porosity of the coal matrix. This model is an extension of a previous work which dealt with pure fluid. Special care is dedicated to keep the model consistent thermodynamically. The model is fully calibrated with a mix of experimental data and numerical data from molecular simulations. Predicting variations of porosity or permeability requires only calibration based on swelling data. With the calibrated state

*Corresponding author. Tel.: +33 (0) 1 81 66 84 44

Email address: patrick.dangla@ifsttar.fr (Patrick Dangla)

equations, we predict numerically how porosity, permeability, and adsorbed amounts of fluid vary in a representative volume element of coal seam in isochoric or oedometric conditions, as a function of the pressure and of the composition of the fluid in the cleats.

Keywords:

poromechanics, competitive adsorption, coal swelling, binary mixtures

1. Introduction

Coal seams are fractured porous media characterized by a relatively large internal surface area of about $30 \text{ m}^2.\text{g}^{-1}$ to $300 \text{ m}^2.\text{g}^{-1}$ [1]. Significant amounts of methane (CH_4) are generated and retained during the geological process leading to their formation, the so-called coalification process [2, 3]. Such coal bed methane (CBM) can be recovered from the coal seam and used for energy production. Conventional primary recovery of methane (called CBM production), which is performed by pumping out water and depressurizing the reservoir, allows producing 20% to 60% of the methane originally present in the reservoir [4]. As is the case with enhanced oil recovery (EOR), such primary production could be in principle enhanced by injecting CO_2 in the coal seam: this process is called CO_2 -Enhanced Coal Bed Methane (CO_2 -ECBM) recovery [4]. Thus, during CO_2 -Enhanced Coal Bed Methane recovery, methane is produced while carbon dioxide is injected. An accurate description of the mixture of CH_4/CO_2 in the coal seam is essential for the development of reliable reservoir simulators used to history match field test data obtained from ECBM field tests [5].

18 Coal seams are naturally fractured by so-called cleats, the opening of
19 which is usually smaller than 0.1 mm at surface conditions [6]. The spacing
20 between those cleats is generally on the order of centimeters [6]. Although
21 the cleat system often occupies less than 1% of the volume of coal [7], this
22 system governs the permeability of the coal seam. Therefore, variations of
23 cleat aperture lead to variations of permeability, which need to be modeled
24 as accurately as possible. In-between those cleats, one finds the coal ma-
25 trix (see Fig. 1), which itself is porous, as it contains both mesopores (i.e.,
26 pores with a diameter comprised between 2 nm and 50 nm) and micropo-
27 res (i.e., pores with a diameter smaller than 2 nm). In such small pores, a
28 significant amount of molecules of the pore fluid are in intermolecular inter-
29 actions with the atoms of the solid skeleton: those molecules are said to be
30 adsorbed. Adsorption confers some specific poromechanical features to the
31 coal matrix: in particular, one observes that coal, when immersed in fluids
32 that can be adsorbed (for instance carbon dioxide or methane), swells [8].
33 This adsorption-induced deformation of the coal matrix leads to variations
34 of the aperture of cleats, which itself translates into variations of permeabil-
35 ity of the coal seam. During CO₂-Enhanced Coal Bed Methane recovery,
36 variations of permeability result therefore from the combination of regular
37 poromechanical effects induced by variations of fluid pressure in the macro-
38 porous cleats with adsorption-induced deformations of the coal matrix [9].
39 Various authors aimed at introducing adsorption-induced swelling effects in
40 coal modeling (for reviews, see [10] and [11]).

41 Deformations induced by adsorption were observed and studied in a va-
42 riety of materials, either mesoporous (e.g., porous silicon [12, 13] or meso-

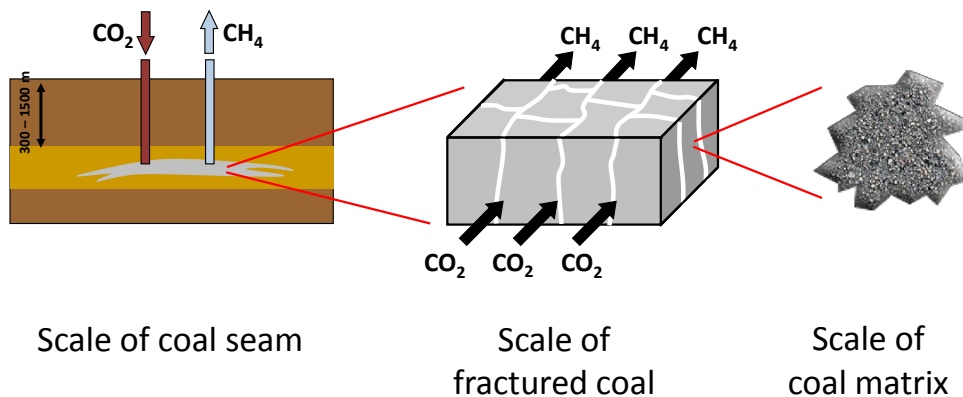


Figure 1: Various scales introduced.

43 porous silica [14, 15, 16, 17]) or microporous (e.g., metal-organic frameworks
 44 [18, 19], zeolites [20], microporous carbons or coal [21, 22, 23]). In meso-
 45 porous solids, adsorption is mostly a surface phenomenon, with adsorbed
 46 molecules located at the surface of the pores. In contrast, in microporous
 47 solids, the very notion of pore surface breaks down and adsorption occurs
 48 by micropore filling rather than by surface covering. The reverse coupling
 49 between adsorption and strain (i.e., the fact that strain or stress can modify
 50 the adsorption process) was also observed. For instance, Grosman and Or-
 51 tega [24, 12] showed the influence of the elastic deformation of porous solids
 52 on the adsorption process: a stress external to the porous layer can modify
 53 the adsorbed amount. Finally, this coupling between strain and adsorption
 54 was also studied for fluid mixtures, for instance in the case of adsorption of
 55 binary mixtures in metal-organic frameworks [25].

56 Based on field and laboratory experimental results, a large variety of permeability relations has been proposed for coal seams (for reviews, see [10] and
 57

58 [11]), starting with the work of Gray [26]. Some models derive such relations
59 by using porosity as an intermediate variable parameter (e.g., [27, 28]) while,
60 in contrast, other models are stress-based (e.g., [29]). Relations were derived
61 for various conditions (e.g., oedometric conditions [28], variable stress con-
62 ditions [30], or triaxial strain or stress conditions [31]). Some models were
63 based on some specific geometries (e.g., a matchstick geometry [32]), or were
64 instead derived for more general geometries by starting from the equations
65 of poroelasticity (e.g., [33]). Liu and Rutqvist [34] considered interaction
66 between adjacent coal matrix blocks through coal matrix bridges. Recently,
67 Liu et al. [35] considered the effect of the transient transfer of fluid between
68 cleats and coal matrix, and Wu et al. [36] derived a poroelastic model aiming
69 at capturing the interactions between binary fluid mixtures (CH_4 and CO_2)
70 and the dual-porosity medium (coal matrix and cleats).

71 Therefore, a large variety of coal models has been developed (for reviews,
72 see [10] and [11]). All these models were derived from the theory of poroe-
73 lasticity or from more empirical continuum approaches. But, while those
74 models focus on how adsorption leads to swelling, only a minority consid-
75 ers the reverse coupling, i.e, how swelling or stresses can modify adsorption,
76 while the fact that compressive stresses can lead to desorption in coal has
77 been shown experimentally [37]. When models do consider such reverse cou-
78 pling (e.g., [38, 22, 39]), they do so by introducing a pore volume of the coal
79 matrix, although defining or measuring the pore volume of a microporous
80 solid such as coal in an unambiguous manner is not possible, since its ap-
81 parent pore volume depends for instance on the fluid with which this pore
82 volume is probed [40]. In contrast, here, we aim at deriving a model with a

83 thermodynamical basis to capture this strong coupling between adsorption
84 and swelling, [without introducing an ill-defined notion of porosity or of pore](#)
85 [volume for the coal matrix: our model is only based on well-defined quanti-](#)
86 [ties](#). Here, a dual-porosity model, based on the Biot-Coussy poromechanical
87 framework [41], is proposed for the behavior of a representative volume el-
88 ement of coal bed reservoir. Both the porous networks of the cleats of the
89 seam and of the coal matrix are explicitly taken into account, [but we never](#)
90 [introduce the pore volume or the porosity of the coal matrix](#). The resulting
91 state equations require directly as an input the adsorption isotherms of the
92 fluids considered on coal and data on adsorption-induced swellings. Recently,
93 we developed a dual-porosity model for coal bed reservoirs, that [considered](#)
94 [adsorption in the coal matrix as a surface phenomenon \[42, 43\]](#). In contrast,
95 [we then developed a model for coal bed reservoirs that also considered the](#)
96 [microporosity of the coal matrix \[44\]](#), in which adsorption occurs by pore
97 filling rather than by surface covering. [In fact, this latter model is valid for a](#)
98 [coal matrix with a generic pore size distribution](#). However, this latter dual-
99 porosity poromechanical model only holds for media saturated with a pure
100 fluid.

101 During ECBM, as the coal bed reservoirs initially contain methane, the
102 injection of carbon dioxide induces a progressive replacement of methane with
103 carbon dioxide. Therefore, here, we develop a dual-porosity model for media
104 exposed to binary mixtures of fluids. We aim at deriving poromechanical
105 equations that model the coupling between adsorption and strains/stresses,
106 and thus enable to predict how the replacement of methane with carbon
107 dioxide leads to strains and variations of porosity or permeability.

108 2. Description of the case considered

109 A representative volume element of coal seam is made of cleats (i.e.,
110 macropores) and of a coal matrix which is potentially microporous (see Fig.
111 1), thus defining two scales: the scale of fractured coal (i.e., a representative
112 volume element of coal seam), and that of the coal matrix.

113 The elastic behavior of the reservoir is considered to be linear and isotropic.
114 Only small strains are considered. The pore space is filled with methane and
115 carbon dioxide, which are assumed to be miscible. The fluid in the cleats is
116 considered to be in a bulk state. Molecules of fluid can be found not only in
117 the cleats, but also in the coal matrix. We assume that fluids in the cleats
118 and in the coal matrix are in equilibrium at all times: the kinetics associated
119 to a transfer of fluid from the cleats to the coal matrix is assumed to be much
120 faster than any other kinetics of the process. Note however that, during the
121 derivation of the state equations, the pressure p of the fluid in the cleats will
122 be considered to be different from the thermodynamic pressure of the fluid
123 in the coal matrix: those two pressures will only be equated at the end of
124 the derivation. Thus, for the derivation, the molar chemical potentials of
125 methane and carbon dioxide in the coal matrix will be considered to differ
126 from the molar chemical potentials of methane and carbon dioxide in the
127 cleats.

128 The bulk mixture of fluid in the cleats is characterized by its pressure p
129 and by its mole fraction x^{CO_2} of carbon dioxide. Alternatively, the state of the
130 fluid in the cleats can be defined through the fugacities f^{CH_4} of methane and
131 f^{CO_2} of carbon dioxide, i.e., $p = p(f^{\text{CO}_2}, f^{\text{CH}_4})$ and $x^{\text{CO}_2} = x^{\text{CO}_2}(f^{\text{CO}_2}, f^{\text{CH}_4})$.

132 If we were to consider a nonporous coal matrix, i.e., with no adsorption

133 effect, the coal seam could be considered as a regular macroporous medium
 134 made of one pore network (i.e., the network of cleats). Therefore, the energy
 135 balance for the nonporous coal matrix in a representative volume element of
 136 coal seam would be [41]:

$$df = \sigma d\epsilon + s_{ij} de_{ij} + pd\phi \quad (1)$$

137 where f is the Helmholtz free energy of the coal matrix per unit volume of
 138 coal seam, σ is the volumetric stress, ϵ is the volumetric strain, s_{ij} are the
 139 deviatoric stresses, e_{ij} are the deviatoric strains, and ϕ is the Lagrangian
 140 porosity of the cleats. Based on this energy balance, one can write the state
 141 equations of the coal seam in absence of any adsorption effect (i.e., for a
 142 nonporous coal matrix) as [41]:

$$d\sigma = (K + b^2 N)d\epsilon - bNd\phi \quad (2)$$

$$dp = -bNd\epsilon + Nd\phi \quad (3)$$

$$ds_{ij} = 2Gde_{ij} \quad (4)$$

143 where K is the drained compression modulus, b is the Biot's coefficient, N
 144 is the Biot's modulus and G the shear modulus [41].

145 **3. Insertion of adsorption effects: case of coal saturated with a** 146 **pure fluid**

147 We now consider a porous coal matrix in contact with a pure fluid: ad-
 148 sorption effects can occur within this matrix. For such coal matrix within a
 149 representative volume element of coal seam, the energy balance is:

$$df = \sigma d\epsilon + s_{ij} de_{ij} + pd\phi + \mu dn, \quad (5)$$

150 where n is the molar fluid content in the coal matrix (i.e., not in the cleats)
 151 per unit volume of undeformed coal seam and μ is the chemical potential of
 152 fluid in the coal matrix. Making use of a Legendre-Fenchel transform, this
 153 energy balance can be rewritten as:

$$d(f - n\mu) = \sigma d\epsilon + s_{ij} de_{ij} + pd\phi - nd\mu, \quad (6)$$

154 from which the state equations in presence of adsorption effects can be in-
 155 ferred in a differential form:

$$d\sigma = (K + b^2 N)d\epsilon - bNd\phi + \alpha_1 d\mu \quad (7)$$

$$dp = -bNd\epsilon + Nd\phi + \alpha_2 d\mu \quad (8)$$

$$ds_{ij} = 2Gde_{ij} \quad (9)$$

$$dn = -\alpha_1 d\epsilon - \alpha_2 d\phi + \alpha_3 d\mu \quad (10)$$

156 where the functions α_1 to α_3 need to be determined. The amount n of fluid
 157 in the coal matrix depends on the chemical potential μ of the fluid in the
 158 coal matrix and on the volume strain ϵ_m of the coal matrix. Using classical
 159 micromechanical relations [41], this volume strain of the coal matrix can be
 160 related to the volume strain ϵ of the coal seam and to the porosity ϕ of the
 161 cleats through:

$$\epsilon = (1 - \phi_0)\epsilon_m + \phi - \phi_0 \quad (11)$$

$$\epsilon_m = \frac{\epsilon - (\phi - \phi_0)}{1 - \phi_0} \quad (12)$$

162 where ϕ_0 is the porosity of the cleats in the state of reference.

163 In addition, since small strains are considered, we can approximate the
 164 adsorbed amount by a first-order expansion with respect to the volume strain
 165 ϵ_m of the coal matrix:

$$n(\mu, \epsilon_m) = (1 - \phi_0) [n_0(\mu) + a(\mu)\epsilon_m] \quad (13)$$

166 where $n_0 + a\epsilon_m$ is the adsorption isotherm per unit volume of undeformed
 167 coal matrix, and where n_0 is the adsorption isotherm on a rigid coal matrix.
 168 Brochard et al. [45] showed by molecular simulations that such expansion is
 169 valid for adsorption of methane in coal for volumetric strains of coal up to 10
 170 %. With this first-order expansion of the adsorption isotherm with respect
 171 to the strain of the coal matrix, we find out that:

$$\alpha_1 = - \left. \frac{\partial n}{\partial \epsilon} \right|_{\phi, \mu} = -(1 - \phi_0)a \left. \frac{\partial \epsilon_m}{\partial \epsilon} \right|_{\phi} = -a \quad (14)$$

172 so that $\alpha_1 = -a(\mu)$. Likewise, we find out that:

$$\alpha_2 = - \left. \frac{\partial n}{\partial \phi} \right|_{\epsilon, \mu} = -(1 - \phi_0)a \left. \frac{\partial \epsilon_m}{\partial \phi} \right|_{\epsilon} = a \quad (15)$$

173 so that $\alpha_2 = -\alpha_1 = a(\mu)$.

174 We note $ad\mu$ as ds^a , where s^a is the volumetric part of an adsorption stress
 175 (from now on referred to as an ‘adsorption stress’) [20, 46], and depends only

176 on the chemical potential of the fluid: $s^a = s^a(\mu)$. Finally, in a differential
 177 form the state equations in presence of adsorption effects are:

$$d\sigma = (K + b^2N)d\epsilon - bNd\phi - ds^a \quad (16)$$

$$dp = -bNd\epsilon + Nd\phi + ds^a \quad (17)$$

$$ds_{ij} = 2Gde_{ij} \quad (18)$$

178 where the small increment ds^a of adsorption stress is given by:

$$ds^a = ad\mu. \quad (19)$$

179 In addition the amount n of fluid in the coal matrix is governed by the
 180 adsorption isotherm (13).

181 It should be noted that this approach does not refer to any particular
 182 size of pores. Unlike cleats, the coal matrix here considered could contain
 183 micropores smaller than 2 nm, the volume of which is ill-defined. Our ap-
 184 proach is then suited for a porous solid with a generic pore size distribution.
 185 The model relies only on the assumed knowledge of the adsorption isotherm,
 186 without referring explicitly to a pore volume or to a pore size distribution.
 187 The apparent density of the adsorbed fluid is likely to differ from the density
 188 ρ of the bulk fluid. It is therefore not possible to assert, as was done for cleats,
 189 that the adsorbed fluid occupies a volume n/ρ in the coal matrix. Indeed,
 190 for very small pores, the apparent density of the adsorbed fluid can differ
 191 significantly from ρ , so that the volume n/ρ can differ significantly from that
 192 of the accommodating coal sample. Therefore, the pore size distribution of
 193 the coal matrix is expected to impact strongly the adsorbed amount n , the

194 coupling coefficient a and thus the adsorption stress s^a .

195 **4. Insertion of adsorption effects: case of coal saturated with a**
196 **mixture of two miscible fluids**

197 We now consider that the coal seam is saturated with a mixture of two
198 miscible fluids: the coal matrix will therefore adsorb a mixture of both fluids.
199 The energy balance for the coal matrix in a representative volume element
200 of coal seam is now:

$$df = \sigma d\epsilon + pd\phi + s_{ij}de_{ij} + \mu^{\text{CH}_4}dn^{\text{CH}_4} + \mu^{\text{CO}_2}dn^{\text{CO}_2}, \quad (20)$$

201 where n^{CH_4} and n^{CO_2} are the amount of methane and carbon dioxide in the
202 coal matrix per unit volume of coal seam, respectively; and where μ^{CH_4} and
203 μ^{CO_2} are the molar chemical potential of methane and carbon dioxide in the
204 coal matrix, respectively. Making use of a Legendre-Fenchel transform, this
205 energy balance can be rewritten as:

$$d(f - n^{\text{CH}_4}\mu^{\text{CH}_4} - n^{\text{CO}_2}\mu^{\text{CO}_2}) = \sigma d\epsilon + s_{ij}de_{ij} + pd\phi - n^{\text{CH}_4}d\mu^{\text{CH}_4} - n^{\text{CO}_2}d\mu^{\text{CO}_2}, \quad (21)$$

206 from which the state equations for a coal seam saturated with a mixture of
207 two fluids can be inferred in a differential form:

$$d\sigma = (K + b^2N)d\epsilon - bNd\phi + \alpha_4d\mu^{\text{CH}_4} + \alpha_5d\mu^{\text{CO}_2} \quad (22)$$

$$dp = -bNd\epsilon + Nd\phi + \alpha_6d\mu^{\text{CH}_4} + \alpha_7d\mu^{\text{CO}_2} \quad (23)$$

$$dn^{\text{CH}_4} = -\alpha_4d\epsilon - \alpha_6d\phi + \alpha_8d\mu^{\text{CH}_4} + \alpha_9d\mu^{\text{CO}_2} \quad (24)$$

$$dn^{\text{CO}_2} = -\alpha_5d\epsilon - \alpha_7d\phi + \alpha_9d\mu^{\text{CH}_4} + \alpha_{10}d\mu^{\text{CO}_2} \quad (25)$$

$$ds_{ij} = 2Gde_{ij}, \quad (26)$$

208 where the functions α_4 to α_{10} need to be determined.

209 Since strains are small, we can approximate the adsorbed amounts by a
210 first-order expansion with respect to the volume strain ϵ_m of the coal matrix:

$$n^{\text{CH}_4}(\epsilon_m, \mu^{\text{CH}_4}, \mu^{\text{CO}_2}) = (1 - \phi_0) (n_0^{\text{CH}_4} + a^{\text{CH}_4}\epsilon_m) \quad (27)$$

$$n^{\text{CO}_2}(\epsilon_m, \mu^{\text{CH}_4}, \mu^{\text{CO}_2}) = (1 - \phi_0) (n_0^{\text{CO}_2} + a^{\text{CO}_2}\epsilon_m), \quad (28)$$

211 where the functions $n_0^{\text{CH}_4}(\mu^{\text{CH}_4}, \mu^{\text{CO}_2})$, $n_0^{\text{CO}_2}(\mu^{\text{CH}_4}, \mu^{\text{CO}_2})$, $a^{\text{CH}_4}(\mu^{\text{CH}_4}, \mu^{\text{CO}_2})$,
212 and $a^{\text{CO}_2}(\mu^{\text{CH}_4}, \mu^{\text{CO}_2})$ all are functions of the chemical potentials only, and
213 where the volume strain ϵ_m of the coal matrix is still related to the porosity
214 ϕ of the cleats and to the volume strain ϵ of the coal seam with Eq. (12).
215 $n_0^{\text{CH}_4} + a^{\text{CH}_4}\epsilon_m$ and $n_0^{\text{CO}_2} + a^{\text{CO}_2}\epsilon_m$ are the adsorption isotherms of methane
216 and carbon dioxide per unit volume of undeformed coal matrix, respectively.
217 $n_0^{\text{CH}_4}$ and $n_0^{\text{CO}_2}$ are the adsorption isotherms of methane and carbon dioxide
218 on a rigid coal matrix, respectively. With these first-order expansions of the
219 adsorption isotherms, we find out that:

$$\alpha_4 = - \left. \frac{\partial n^{\text{CH}_4}}{\partial \epsilon} \right|_{\phi, \mu^{\text{CH}_4}, \mu^{\text{CO}_2}} = -(1 - \phi_0)a^{\text{CH}_4} \left. \frac{\partial \epsilon_m}{\partial \epsilon} \right|_{\phi} = -a^{\text{CH}_4}, \quad (29)$$

220 so that $\alpha_4 = -a^{\text{CH}_4}(\mu^{\text{CH}_4}, \mu^{\text{CO}_2})$. Likewise, we find out that:

$$\alpha_6 = - \left. \frac{\partial n^{\text{CH}_4}}{\partial \phi} \right|_{\epsilon, \mu^{\text{CH}_4}, \mu^{\text{CO}_2}} = -(1 - \phi_0) a^{\text{CH}_4} \left. \frac{\partial \epsilon_m}{\partial \phi} \right|_{\epsilon} = a^{\text{CH}_4}, \quad (30)$$

221 so that $\alpha_6 = -\alpha_4 = a^{\text{CH}_4}(\mu^{\text{CH}_4}, \mu^{\text{CO}_2})$.

222 We also find out that:

$$\alpha_5 = \alpha_5(\mu^{\text{CH}_4}, \mu^{\text{CO}_2}) = -a^{\text{CO}_2} \quad (31)$$

$$\alpha_7 = \alpha_7(\mu^{\text{CH}_4}, \mu^{\text{CO}_2}) = a^{\text{CO}_2}. \quad (32)$$

The function $a^{\text{CH}_4} d\mu^{\text{CH}_4} + a^{\text{CO}_2} d\mu^{\text{CO}_2}$ can be rewritten as a small increment ds^a of adsorption stress:

$$ds^a = a^{\text{CH}_4} d\mu^{\text{CH}_4} + a^{\text{CO}_2} d\mu^{\text{CO}_2}, \quad (33)$$

223 which was inferred from the Maxwell symmetry relationship derived from

224 Eq. (22):

$$-\frac{\partial^2 \sigma}{\partial \mu^{\text{CH}_4} \partial \mu^{\text{CO}_2}} = \left. \frac{\partial a^{\text{CH}_4}}{\partial \mu^{\text{CO}_2}} \right|_{\mu^{\text{CH}_4}} = \left. \frac{\partial a^{\text{CO}_2}}{\partial \mu^{\text{CH}_4}} \right|_{\mu^{\text{CO}_2}}. \quad (34)$$

225 In such a case, finally, in a differential form the state equations of a coal

226 seam in presence of a binary mixture of fluids are:

$$d\sigma = (K + b^2 N) d\epsilon - bN d\phi - ds^a \quad (35)$$

$$dp = -bN d\epsilon + N d\phi + ds^a \quad (36)$$

$$ds_{ij} = 2G de_{ij} \quad (37)$$

227 where the small increment ds^a of adsorption stress is given by:

$$ds^a = a^{\text{CH}_4} d\mu^{\text{CH}_4} + a^{\text{CO}_2} d\mu^{\text{CO}_2} \quad (38)$$

228 In addition the amounts n^{CH_4} and n^{CO_2} of fluid in the coal matrix are given
 229 by Eqs. (27)-(28), respectively.

230 As was the case for a coal seam saturated with a pure fluid, adsorption
 231 effects for a coal seam saturated with a mixture of two miscible fluids can be
 232 captured by the introduction of an adsorption stress s^a . Moreover, one notes
 233 that the state equations (35)-(37) derived for a coal seam saturated with a
 234 mixture of two miscible fluids are strictly identical to the state equations
 235 (16)-(18) derived for a coal seam saturated with a pure fluid. However, while
 236 a small increment ds^a of adsorption stress is given by Eq. (19) when coal is
 237 saturated with a pure fluid, this same small increment ds^a is given by Eq.
 238 (38) when coal is saturated with a mixture of two miscible fluids. *Let us*
 239 *point out that this result is obtained without referring to an ideality of the*
 240 *mixture of CH₄ and CO₂ since the chemical potentials of these gases in the*
 241 *mixture are general and do not refer to any specific model. However, the*
 242 *derivation of the adsorption stress, as resulting from a total exact differential*
 243 *form, relies on the assumption that the gas contents are linearly linked to*
 244 *the strain (see Eqs. (27) and (28)).*

245 Thermodynamic equilibrium of each fluid found in the cleats and in the
 246 coal matrix is now introduced. Equating the chemical potentials in differen-
 247 tial form yields:

$$d\mu^{\text{CH}_4} = RT \frac{df^{\text{CH}_4}}{f^{\text{CH}_4}} \quad (39)$$

$$d\mu^{\text{CO}_2} = RT \frac{df^{\text{CO}_2}}{f^{\text{CO}_2}}, \quad (40)$$

248 with T the temperature and R the ideal gas constant, so that, eventually,
 249 $\mu^{\text{CH}_4} = \mu^{\text{CH}_4}(f^{\text{CH}_4}) = \mu^{\text{CH}_4}(p, x^{\text{CO}_2})$ and $\mu^{\text{CO}_2} = \mu^{\text{CO}_2}(f^{\text{CO}_2}) = \mu^{\text{CO}_2}(p, x^{\text{CO}_2})$.

250 **5. Application to coal saturated with a mixture of CH₄ and CO₂**

251 Based on the derivations performed in the previous section, one can pre-
 252 dict how various parameters such as cleat porosity or permeability evolve
 253 for a representative volume element of coal seam saturated by a mixture of
 254 two fluids, as will be explained in Sec. 5.2. In addition, a salient feature
 255 of our model is that it captures the full coupling between adsorption and
 256 stresses/strains: not only does it make it possible to predict how stresses or
 257 strains evolve in presence of adsorption, but also does it make it possible to
 258 predict how stresses or strains affect adsorption, as will be presented in the
 259 section after. As a prerequisite to those calculations, the adsorption stress
 260 s^a that develops when cleats are occupied by a mixture of fluids must be
 261 calculated, which is the focus of the next section.

262 The properties of the coal here considered are given in Table 1. All
 263 properties are characteristic of coal.

264 *5.1. Calculation of adsorption stress*

265 This section is dedicated to calculating the adsorption stress s^a for a
 266 specific coal. Since the cleat porosity is occupied by a mixture of methane

Table 1: Parameters of the coal of interest. For values not provided by Pini et al. [47], a typical range of values is indicated. Values from a) [47], b) [48], c) [7], d) [49], e) [50]. The bulk modulus K_m of the coal matrix and the Biot modulus N are calculated with the following relations [41]: $b = 1 - K/K_m$ and $1/N = (b - \phi_0)/K_m$.

Property	Definition, Unit	Value	Typical range of values
K	Bulk modulus of coal sample, GPa	0.78 ^{a)}	
b	Biot coefficient of coal sample	0.75	[0:1] ^{b)}
K_m	Bulk modulus of coal matrix, GPa	3.12	
ϕ_0	Initial porosity of cleats	3.2% ^{a)}	
N	Biot modulus, GPa	4.22	
γ	Pressure sensitivity parameter, MPa ⁻¹	0.15	[0.04 ^{d)} :0.9 ^{e)}

267 and carbon dioxide, this adsorption stress depends on both the pressure p of
 268 the mixture in the cleats and on the mole fraction x^{CO_2} of carbon dioxide in
 269 this mixture, i.e.:

$$s^a(p, x^{\text{CO}_2}) = s^a(f^{\text{CH}_4}, f^{\text{CO}_2}) \quad (41)$$

270 where f^{CH_4} and f^{CO_2} are the fugacities of methane and carbon dioxide in the
 271 mixture that saturates the cleats, respectively. Since we assume thermody-
 272 namic equilibrium between cleats and coal matrix, those fugacities are also
 273 those of methane and carbon dioxide in the coal matrix. However, because
 274 of adsorption, the mole fraction of carbon dioxide in the coal matrix is likely
 275 to differ from the mole fraction x^{CO_2} of carbon dioxide in the cleats [45].

276 We first perform some simplification, while aiming at keeping the thermo-
 277 dynamic consistency of the model, i.e., at being consistent with the following
 278 equation obtained by a combination of Eq. (38) with Eqs. (39)-(40):

$$ds^a = RT \left[a^{\text{CH}_4} \frac{df^{\text{CH}_4}}{f^{\text{CH}_4}} + a^{\text{CO}_2} \frac{df^{\text{CO}_2}}{f^{\text{CO}_2}} \right]. \quad (42)$$

279 From the lack of knowledge, we assume that the coefficients a^{CH_4} and
 280 a^{CO_2} are of the form:

$$a^{\text{CH}_4}(p, x^{\text{CO}_2}) = a^{\text{CH}_4}(f^{\text{CH}_4}) \quad (43)$$

$$a^{\text{CO}_2}(p, x^{\text{CO}_2}) = a^{\text{CO}_2}(f^{\text{CO}_2}). \quad (44)$$

281 With such an assumption, the compatibility equation (34) is readily enforced,
 282 which enables to ensure that the thermodynamic consistency of the model is
 283 conserved.

284 The fugacities of pure methane and pure carbon dioxide are noted $f_*^{\text{CH}_4}$
 285 and $f_*^{\text{CO}_2}$, respectively. Those fugacities, calculated from the NIST thermo-
 286 physical properties of fluid systems (<http://webbook.nist.gov/chemistry/>),
 287 are displayed in Fig. 2a. From molecular simulations of bulk binary mix-
 288 tures of methane and carbon dioxide [45] (see Fig. 2b), one observes that,
 289 in first-order approximation, the fugacities f^{CO_2} of carbon dioxide and f^{CH_4}
 290 of methane in the mixture can be linked to the fugacities $f_*^{\text{CO}_2}$ of pure car-
 291 bon dioxide and $f_*^{\text{CH}_4}$ of pure methane at the same pressure as the mixture
 292 through:

$$f^{\text{CH}_4} = f_*^{\text{CH}_4} (1 - x^{\text{CO}_2}) \quad (45)$$

$$f^{\text{CO}_2} = f_*^{\text{CO}_2} x^{\text{CO}_2}. \quad (46)$$

293 Those equations state that the binary mixture follows a Raoult's law, i.e.,
 294 that the chemical potentials of methane and carbon dioxide in the mixture

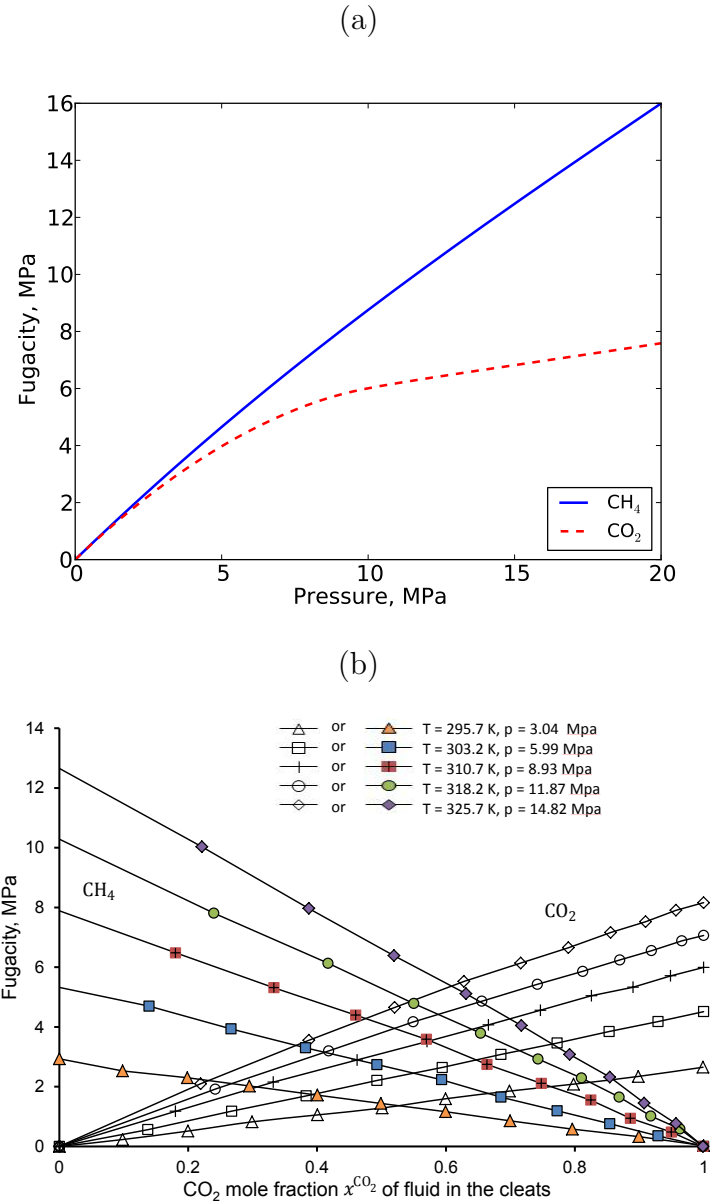


Figure 2: (a) Fugacity $f_*^{\text{CO}_2}$ of pure carbon dioxide and $f_*^{\text{CH}_4}$ of pure methane at a temperature $T = 318.15 \text{ K}$, adapted from the NIST thermophysical properties of fluid systems (<http://webbook.nist.gov/chemistry/>). (b) Fugacity f^{CH_4} of methane and f^{CO_2} of carbon dioxide in the CH_4 - CO_2 mixture, as a function of the pressure, temperature and composition of the mixture, adapted from molecular simulations by Brochard et al. [45]. Open symbols are for CO_2 while filled symbols are for CH_4 .

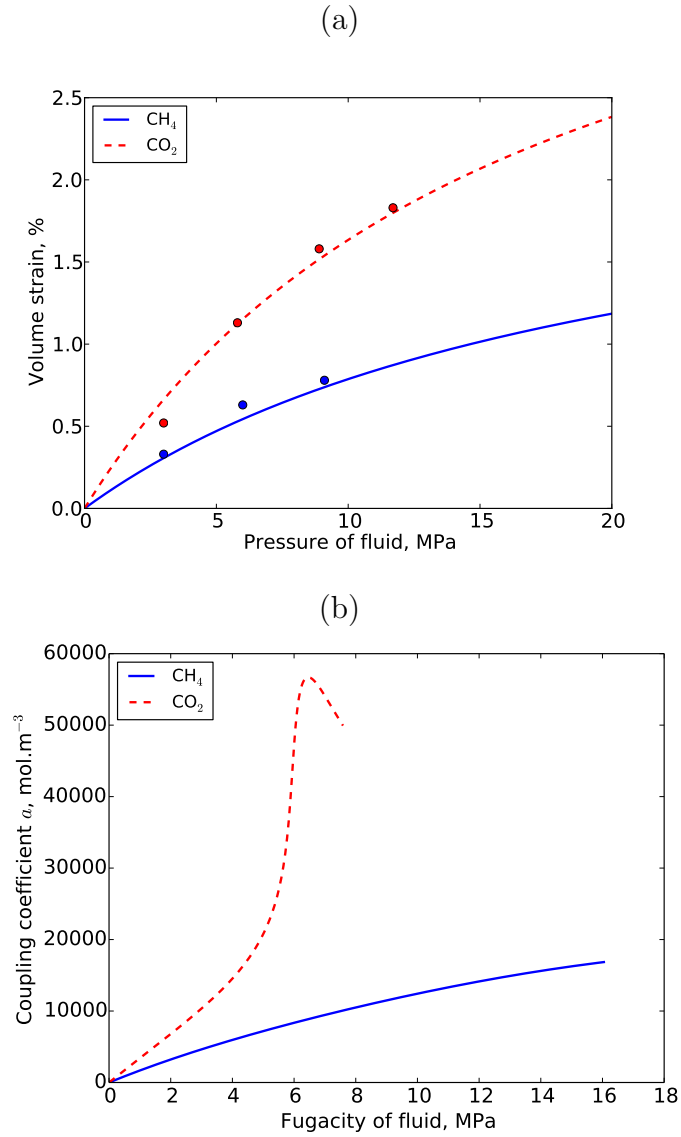


Figure 3: (a) Volume strain of Ribolla coal sample immersed in pure methane or pure carbon dioxide at a temperature $T = 318.15$ K. Data is adapted from Pini et al. [51]. Symbols are data points while lines are models fitted by Pini et al. on their data. (b) Functions a^{CH_4} and a^{CO_2} that govern how strain modifies adsorption (see Eqs. (27)-(28)).

295 are given by $\mu^{\text{CH}_4} = \mu_*^{\text{CH}_4} + RT \ln(1 - x^{\text{CO}_2})$ and $\mu^{\text{CO}_2} = \mu_*^{\text{CO}_2} + RT \ln(x^{\text{CO}_2})$.
 296 The bulk mixture is therefore assumed as ideal here. This assumption is
 297 supported by observations in a first approximation as shown in Fig. 2, even
 298 though a more accurate observation of these curves shows a slight departure
 299 from ideality.

300 Under the above assumptions, we will show that the only data required to
 301 calculate the adsorption stress in presence of a mixture are data of swelling of
 302 coal samples in presence of the pure fluids. We will use swelling strains data
 303 obtained by Pini [51] for Ribolla coal in presence of pure methane or pure
 304 carbon dioxide at a temperature $T = 318.15$ K. Their data are displayed
 305 in Fig. 3a. The strains of coal samples immersed in pure methane or in
 306 pure carbon dioxide are noted ϵ^{CH_4} and ϵ^{CO_2} , respectively. Considering the
 307 state equations (16) and (17) for a sample immersed in a fluid (i.e., for which
 308 $\sigma = -p$), independently of the initial porosity ϕ_0 of the cleats, one finds
 309 out that the coupling coefficients a^{CH_4} and a^{CO_2} are linked to the measured
 310 swelling strains through:

$$a^{\text{CH}_4}(f_*^{\text{CH}_4}) = \rho^{\text{CH}_4} \left(1 + K_m \frac{d\epsilon^{\text{CH}_4}}{dp} \right) \text{ and } a^{\text{CO}_2}(f_*^{\text{CO}_2}) = \rho^{\text{CO}_2} \left(1 + K_m \frac{d\epsilon^{\text{CO}_2}}{dp} \right), \quad (47)$$

311 where ρ^{CH_4} and ρ^{CO_2} are the bulk densities of methane and carbon dioxide,
 312 respectively, and where K_m is the bulk modulus of the coal matrix. Thus, the
 313 functions $a^{\text{CH}_4}(f_*^{\text{CH}_4})$ and $a^{\text{CO}_2}(f_*^{\text{CO}_2})$ can be identified with the equations
 314 (47) derived for pure fluids. The results of those calculations based on the
 315 data obtained by Pini [51] are displayed in Fig. 3b. In this figure, the coupling
 316 coefficient obtained for CO_2 shows a peak resulting from the competition

317 between two contrasting behaviors. We can show that $a = \rho(ds^a/dp)$, where
 318 the gas density ρ is an increasing function of pressure, and where ds^a/dp is
 319 a decreasing function of pressure [44]. It turns out that the derivative of a
 320 with respect to fugacity is dominated by that of ρ for small pressures and by
 321 that of ds^a/dp for high pressures (actually supercritical pressures).

322 The functions a^{CH_4} and a^{CO_2} being now known, the adsorption stress s^a
 323 can be calculated with the help of Eq. (38):

$$ds^a(p, x^{\text{CO}_2}) = a^{\text{CH}_4}d\mu^{\text{CH}_4} + a^{\text{CO}_2}d\mu^{\text{CO}_2} \quad (48)$$

$$= RT \left[\frac{a^{\text{CH}_4}(f^{\text{CH}_4})}{f^{\text{CH}_4}} df^{\text{CH}_4} + \frac{a^{\text{CO}_2}(f^{\text{CO}_2})}{f^{\text{CO}_2}} df^{\text{CO}_2} \right] \quad (49)$$

324 or, in an integrated form:

$$s^a(p, x^{\text{CO}_2}) = RT \left[\int_0^{f^{\text{CH}_4}} \frac{a^{\text{CH}_4}(\tilde{f}^{\text{CH}_4})}{\tilde{f}^{\text{CH}_4}} d\tilde{f}^{\text{CH}_4} + \int_0^{f^{\text{CO}_2}} \frac{a^{\text{CO}_2}(\tilde{f}^{\text{CO}_2})}{\tilde{f}^{\text{CO}_2}} d\tilde{f}^{\text{CO}_2} \right] \quad (50)$$

$$= RT \left[\int_0^{f_*^{\text{CH}_4} x^{\text{CH}_4}} \frac{a^{\text{CH}_4}(\tilde{f}^{\text{CH}_4})}{\tilde{f}^{\text{CH}_4}} d\tilde{f}^{\text{CH}_4} + \int_0^{f_*^{\text{CO}_2} x^{\text{CO}_2}} \frac{a^{\text{CO}_2}(\tilde{f}^{\text{CO}_2})}{\tilde{f}^{\text{CO}_2}} d\tilde{f}^{\text{CO}_2} \right] \quad (51)$$

325 Here, the adsorption stress $s^a(p, x^{\text{CO}_2})$ was calculated based on the exper-
 326 imental data obtained for pure methane and pure carbon dioxide on Ribolla
 327 coal at a temperature $T = 318.15$ K (see Fig. 3a) and on the fugacities
 328 of pure methane and pure carbon dioxide obtained from the NIST thermo-
 329 physical properties of fluid systems (<http://webbook.nist.gov/chemistry/>) at
 330 the same temperature (see Fig. 2a). Fig. 4 displays the adsorption stress

331 $s^a(p, x^{\text{CO}_2})$ for various values of the mole fraction x^{CO_2} of carbon dioxide in
 332 the fluid mixture in the cleats and for various pressures p of this mixture.
 333 Fig. 4 shows that variations of the adsorption stress $s^a(p, x^{\text{CO}_2})$ are non triv-
 334 ial. This adsorption stress increases with the pressure p of the mixture in
 335 the cleats. The adsorption stress also increases with the mole fraction of
 336 carbon dioxide in a way depending on the pressure level. At low pressure the
 337 fugacities of the two gases are small enough for the coupling coefficient to
 338 be approximated by a first-order expansion of the fugacity. It turns out that
 339 the adsorption stress is linearly linked to the mole fraction. At high pressure,
 340 namely close to the critical point of CO_2 , the coupling coefficient relative to
 341 CO_2 is no more linearly linked to the fugacity, as shown in Fig. 3b. As a
 342 consequence, the adsorption stress presents a nonlinear behavior for a large
 343 enough CO_2 mole fraction, as shown in Fig. 4b.

344 *5.2. Prediction of variations of porosity and permeability for sample in iso-*
 345 *choric conditions*

346 The knowledge of this adsorption stress now makes it possible to use the
 347 state equations (35)-(37). In this section, we focus on a representative volume
 348 element of coal seam kept in isochoric conditions, i.e., $\epsilon = 0$. Among others,
 349 the state equations enable to calculate variations of porosity:

$$\phi - \phi_0 = \frac{1}{N}(p - s^a) \quad (52)$$

350 The calculated variations of porosity are displayed in Fig. 5. One ob-
 351 serves that, in the range of pressures considered, for a given composition of
 352 the mixture in the cleats, any increase of pressure in the cleats translates into

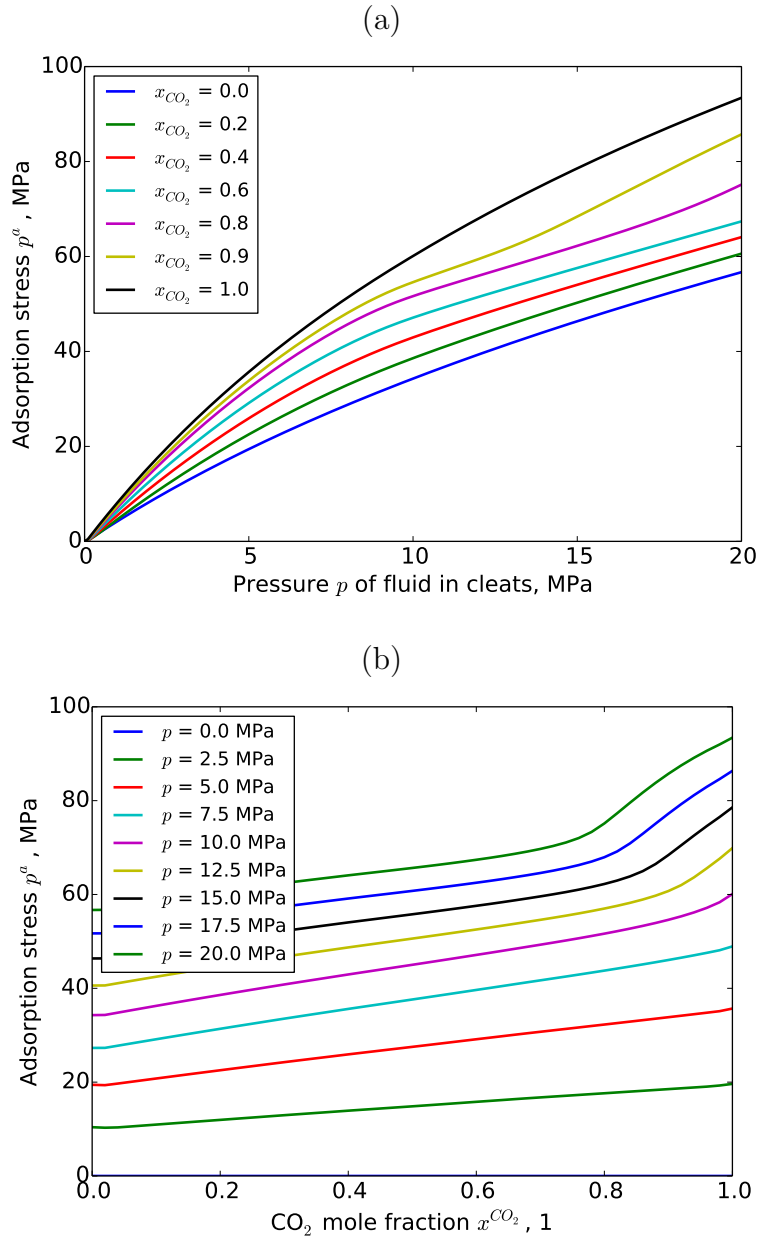


Figure 4: Adsorption stress $s^a(p, x^{\text{CO}_2})$ for Ribolla coal sample exposed to a mixture of methane and carbon dioxide at a temperature $T = 318.15$ K versus (a) the pressure p of the fluid in the cleats and (b) the mole fraction x^{CO_2} of carbon dioxide in the fluid mixture in the cleats.

353 a decrease of the porosity ϕ of the cleats: this phenomenon is a direct conse-
 354 quence of the swelling of the coal matrix upon increasing pressure of fluid. In
 355 contrast, at a given pressure of the mixture in the cleats, how the porosity of
 356 the cleats evolves with the composition of the mixture is non trivial. At the
 357 lowest pressures considered, porosity is almost related in an affine manner to
 358 the mole fraction x^{CO_2} of carbon dioxide in the mixture in the cleats. How-
 359 ever, at the largest pressures here considered, the relation between porosity
 360 and mole fraction becomes significantly nonlinear: at pressures comprised
 361 between roughly 15 MPa and 20 MPa, most decrease of the porosity occurs
 362 for CO_2 mole fractions greater than 0.8. This behavior reflects the behavior
 363 of the adsorption stress as described previously.

364 After some modification, the state equations (35)-(37) also make it pos-
 365 sible to calculate variations of permeability. Indeed, classically for coal, the
 366 following stress-based permeability relation is considered [52]:

$$k = k_0 \exp(\gamma(\sigma + p)) \quad (53)$$

367 where γ is the so-called pressure sensitivity parameter, first introduced by
 368 Brace et al. [53], and where $\sigma + p$ is the Terzaghi's effective stress. Combining
 369 this equation with the state equations (35)-(37) enables to find out how
 370 permeability is related to the adsorption stress s^a for a representative volume
 371 element of coal seam kept in isochoric conditions:

$$k = k_0 \exp(\gamma(1 - b)(p - s^a)) \quad (54)$$

372 where $b = 1 - K/K_m$ is the Biot coefficient of the coal seam.

373 Knowing the adsorption stress, this equation makes it possible to calculate

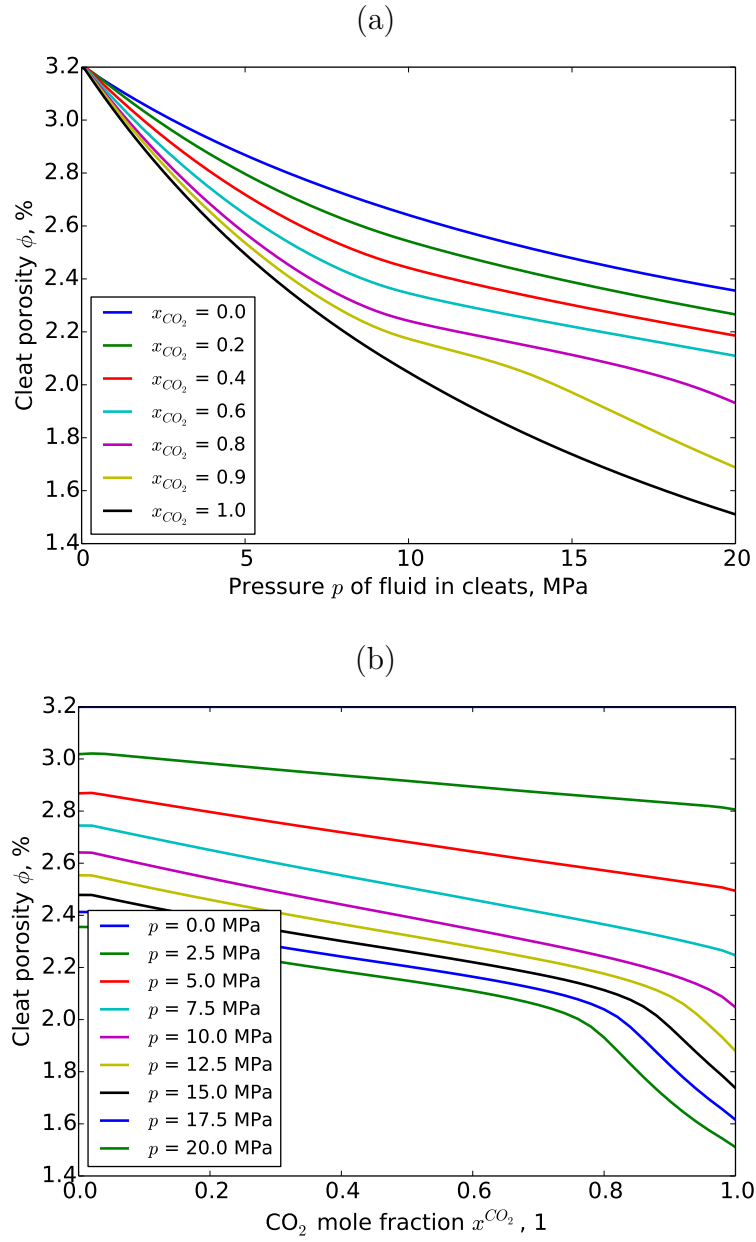


Figure 5: Variations of cleat porosity ϕ of a Ribolla coal sample in isochoric conditions, exposed to a mixture of methane and carbon dioxide at a temperature $T = 318.15$ K versus (a) the pressure p of the fluid in the cleats and (b) the mole fraction x^{CO_2} of carbon dioxide in the fluid mixture in the cleats.

374 variations of permeability, as displayed in Fig. 6. One observes that the
375 variations of permeability, when displayed on a logarithmic scale, are very
376 similar to the variations of porosity (see Fig. 5).

377 The calculations in this section were performed for a representative vol-
378 ume element in isochoric conditions, which, with free swelling conditions,
379 represent two extreme cases. In free swelling conditions, the model predicts
380 no variation of the Terzaghi's effective stress and thus no variation of per-
381 meability. Also, in free swelling conditions, the model predicts a homothetic
382 swelling of the porous solid, from what follows that the pore volume varies
383 such that the Eulerian porosity remains constant.

384 *5.3. Variations of adsorbed amount*

385 In addition to the calculations presented in the previous sections, since
386 the model we propose is fully coupled, predicting the amounts of adsorbed
387 fluids in various conditions is possible. As we will see, taking into account this
388 coupling can lead to significant differences. Here we focus on two identical
389 representative volume elements of coal seam: one element is kept in isochoric
390 conditions, while the other is allowed to swell freely.

391 Here, in addition to the functions a^{CH_4} and a^{CO_2} already calibrated, ad-
392 sorption isotherms need to be known and calibrated. Again, for the cases of
393 pure fluids, we will use the data of Pini et al. [54], who provide adsorption
394 isotherms of pure methane and pure carbon dioxide on Ribolla coal. Those
395 adsorption isotherms, expressed in terms of total amounts of fluid, are dis-
396 played in Fig. 7. By construction, the isotherms provided by Pini et al.
397 converge toward a finite value at infinite pressures, and we therefore inter-
398 pret them as isotherms representative of isotherms on a rigid coal matrix:

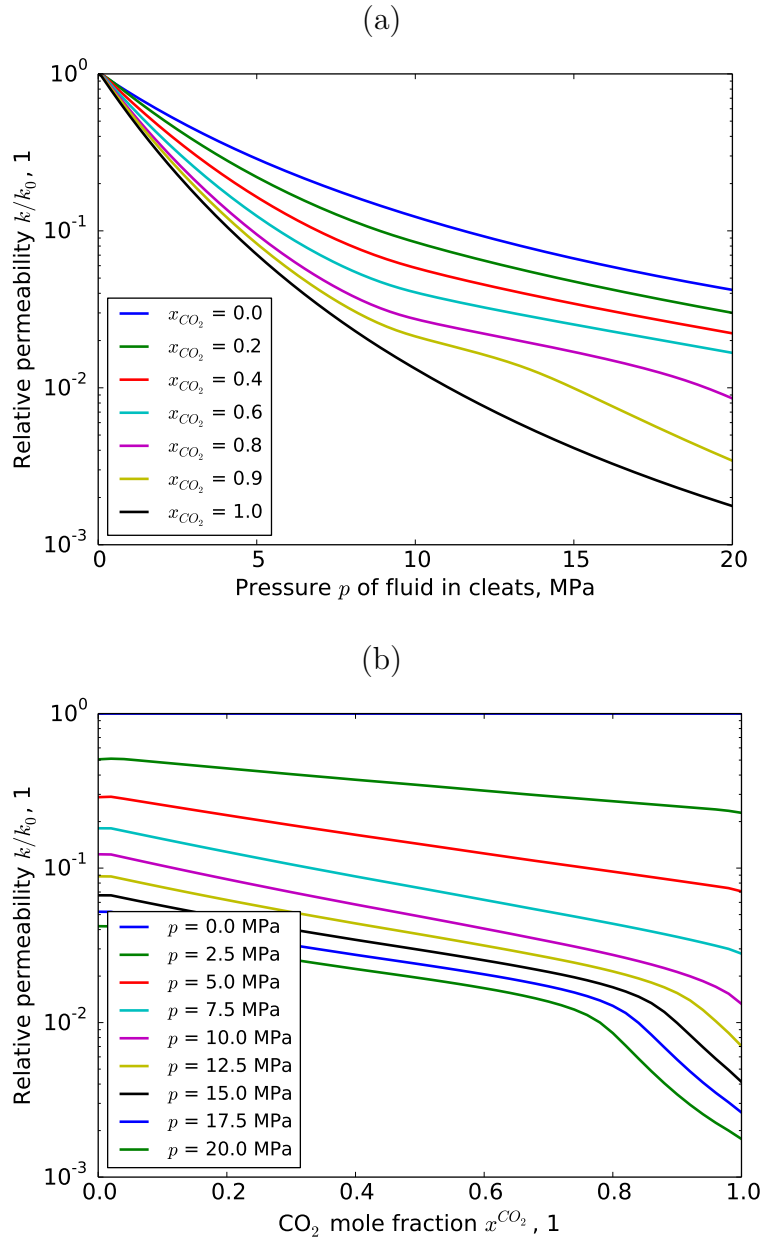


Figure 6: Variations of permeability k of a Ribolla coal sample in isochoric conditions, exposed to a mixture of methane and carbon dioxide at a temperature $T = 318.15$ K versus (a) the pressure p of the fluid in the cleats and (b) the mole fraction x^{CO_2} of carbon dioxide in the fluid mixture in the cleats.

399 thus, those isotherms are those noted $n_0^{\text{CH}_4}(p, x^{\text{CO}_2} = 0)$ for pure methane
 400 and $n_0^{\text{CO}_2}(p, x^{\text{CO}_2} = 1)$ for pure carbon dioxide.

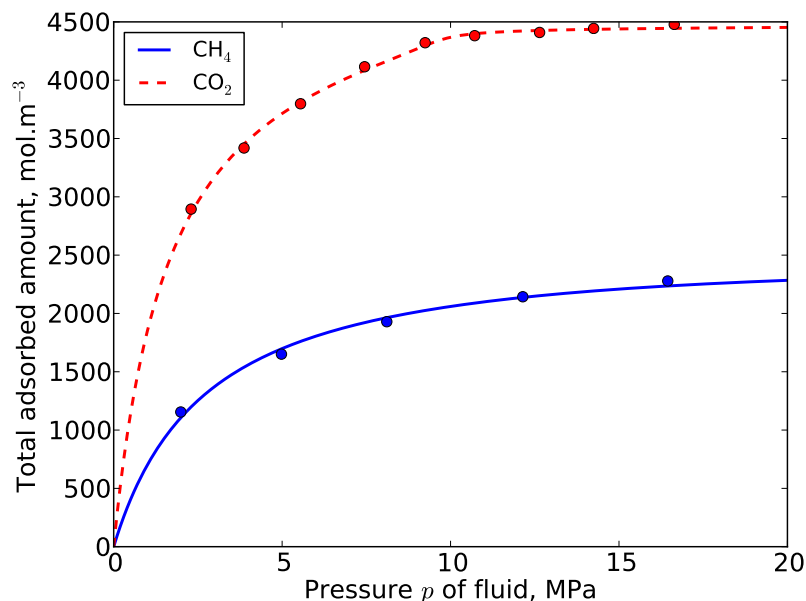


Figure 7: Adsorbed amounts of pure fluids in Ribolla coal at a temperature $T = 318.15$ K, adapted from Pini et al. [54]. Symbols are data points while lines are models fitted by Pini et al. on their data.

401 In contrast to data of adsorption of pure fluids, data of adsorption of
 402 mixtures of fluids are difficult to obtain experimentally, not only because
 403 of the complexity of the required experimental setup, but also because of
 404 the duration of the corresponding experiments. For our specific problem,
 405 as an alternative, we aim at using numerical adsorption isotherms obtained
 406 by molecular simulations by Brochard et al. [45]. In particular, Brochard
 407 et al. [45] obtained numerical data of adsorbed amounts of both methane

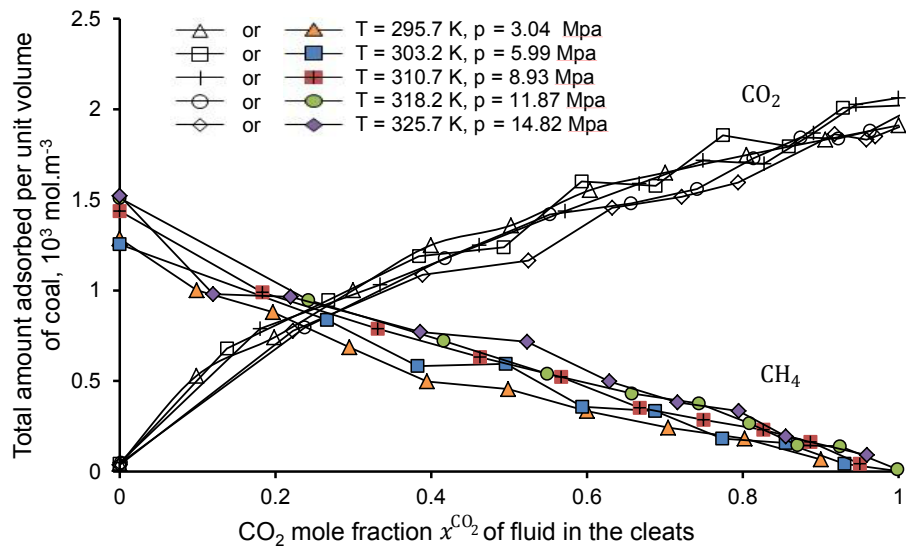


Figure 8: Total amounts of methane and carbon dioxide adsorbed in a rigid coal sample exposed to a mixture of methane and carbon dioxide, adapted from [molecular simulations by Brochard et al. \[45\]](#). Open symbols are for CO₂ while filled symbols are for CH₄. The CO₂ mole fraction x^{CO_2} is that in a reservoir in thermodynamic equilibrium with the sample (i.e., in our case, of the fluid mixture in the cleats).

408 and carbon dioxide when a rigid piece of coal matrix is exposed to a mixture
 409 of methane and carbon dioxide that contains various mole fractions x^{CO_2} of
 410 carbon dioxide, at various temperatures and pressures. Their results are dis-
 411 played in Fig. 8. From this figure, it appears that the relative amounts of
 412 methane and carbon dioxide in the coal matrix depend mostly on the com-
 413 position of the fluid in thermodynamical equilibrium with the coal matrix.
 414 Therefore, we will approximate the mixed adsorption isotherms $n_0^{\text{CH}_4}(p, x^{\text{CO}_2})$
 415 and $n_0^{\text{CO}_2}(p, x^{\text{CO}_2})$ by:

$$n_0^{\text{CH}_4}(p, x^{\text{CO}_2}) = n_0^{\text{CH}_4}(p, x^{\text{CO}_2} = 0)g^{\text{CH}_4}(x^{\text{CO}_2}) \quad (55)$$

$$n_0^{\text{CO}_2}(p, x^{\text{CO}_2}) = n_0^{\text{CO}_2}(p, x^{\text{CO}_2} = 1)g^{\text{CO}_2}(x^{\text{CO}_2}) \quad (56)$$

416 where $n_0^{\text{CH}_4}(p, x^{\text{CO}_2} = 0)$ and $n_0^{\text{CO}_2}(p, x^{\text{CO}_2} = 1)$ are the adsorption isotherms
 417 of pure methane and pure carbon dioxide on a rigid coal matrix, respec-
 418 tively, and where $g^{\text{CH}_4}(x^{\text{CO}_2})$ and $g^{\text{CO}_2}(x^{\text{CO}_2})$ are functions. Those last two
 419 functions can readily be obtained from Fig. 8: here those functions are calcu-
 420 lated based on the results of Brochard et al. at 318.2 K. Eqs. (55-56) should
 421 be considered as the best proposed approximations of the mixed adsorption
 422 isotherms that we can make up to now. In absence of any experimental
 423 data reported in the literature, these expressions are only supported by re-
 424 sults of molecular simulations performed by Brochard et al. [45]. Moreover
 425 and unfortunately we were unable to support these approximations by some
 426 physical background.

427 Therefore, making use of Eqs. (27)-(28), the amounts of fluid in the coal
 428 matrix can be calculated with:

$$n^{\text{CH}_4}(\epsilon_m, p, x^{\text{CO}_2}) = (1 - \phi_0) (n_0^{\text{CH}_4}(p, x^{\text{CO}_2}) + a^{\text{CH}_4}(f^{\text{CH}_4})\epsilon_m) \quad (57)$$

$$n^{\text{CO}_2}(\epsilon_m, p, x^{\text{CO}_2}) = (1 - \phi_0) (n_0^{\text{CO}_2}(p, x^{\text{CO}_2}) + a^{\text{CO}_2}(f^{\text{CO}_2})\epsilon_m) \quad (58)$$

429 where the fugacities f^{CH_4} of methane and f^{CO_2} of carbon dioxide are given
 430 by Eqs. (45)-(46), the functions a^{CH_4} and a^{CO_2} by Eqs. (47), and x^{CO_2} is the
 431 CO_2 mole fraction of the fluid in the cleats.

432 Based on those equations, we calculate the amount of fluid in the coal
 433 matrix of a representative volume element of coal seam for two loading paths:
 434 the representative volume element is kept in isochoric conditions or is allowed
 435 to swell freely. The results of the calculation are displayed in Fig. 9. As
 436 expected, for a given composition of mixture, independent of the loading
 437 path, increasing the pressure of the fluid in the cleats always increases the
 438 total amount of fluid in the coal matrix. Also, one observes that the ad-
 439 sorbed amount depends on the loading path: at the greatest pressure here
 440 considered, depending on the composition of the mixture, considering one
 441 type of loading or the other can make the total amount of carbon dioxide
 442 vary by about 10%. This calculation shows that the effect of deformation
 443 on the adsorbed amount must be explicitly taken into account, as our model
 444 proposes.

445 Note finally that the total amount of fluid in the coal seam per unit
 446 volume of coal seam (this amount is noted $n_T^{\text{CH}_4}$ for methane and $n_T^{\text{CO}_2}$ for
 447 carbon dioxide) is equal to the addition of the amount in the coal matrix
 448 with the amount of fluid in the cleats:

$$n_T^{\text{CH}_4} = n^{\text{CH}_4} + \rho^{\text{CH}_4}\phi \text{ and } n_T^{\text{CO}_2} = n^{\text{CO}_2} + \rho^{\text{CO}_2}\phi. \quad (59)$$

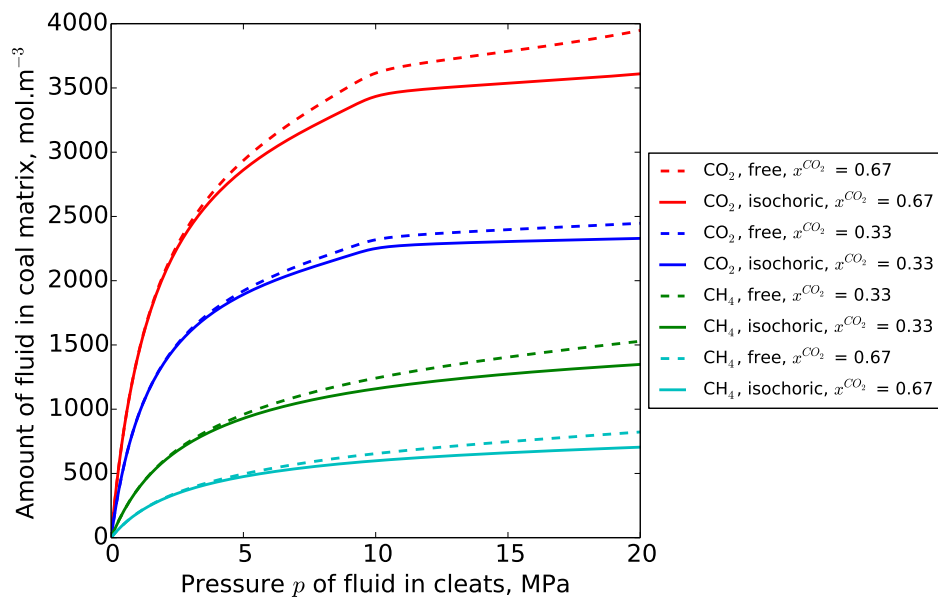


Figure 9: Predicted amounts of methane and carbon dioxide in the coal matrix, for a representative volume element of coal seam injected with a binary mixture of fluids with various compositions and pressures, and kept in isochoric conditions or allowed to swell freely.

449 where ρ^{CH_4} and ρ^{CO_2} are the bulk densities of methane and carbon dioxide,
450 respectively.

451 **6. Concluding remarks**

452 In this work, the poromechanical model derived in Nikoosokhan et al. [44]
453 for coal exposed to a pure fluid was extended to coal exposed to a binary mix-
454 ture. Some assumptions were needed in order to obtain a thermodynamically
455 consistent model that could be fully calibrated with available data. Those
456 assumptions are on the consideration of small strains (see Eqs. (27)-(28)),
457 on the shape of the adsorption isotherms of mixtures (see Eqs. (55)-(56)),
458 and on the dependency of the introduced functions a^{CH_4} and a^{CO_2} (see Eqs.
459 (43)-(44)) on the fugacities of the fluids in the mixture.

460 We showed that calculating permeability and porosity evolutions only
461 required data of adsorption-induced swellings in presence of pure fluids for
462 the model to be calibrated. In contrast, calculating adsorbed amounts on
463 deformed samples required to know data of adsorption-induced swellings with
464 pure fluids and isotherms of adsorption and co-adsorption. Here we used
465 swelling data and adsorption data with pure fluids obtained experimentally,
466 while we used data obtained by molecular simulations for the co-adsorption
467 isotherms (see Figs. 3a and 7).

468 One feature of our model is that it captures the full coupling between
469 adsorption and stress/strain: not only does it model the fact that adsorption
470 generates adsorption stresses (or strains), but also does it model the fact
471 that adsorption is modified by the stresses or strains to which the solid is
472 subjected. By performing calculations on a [representative volume element](#)

473 of coal seam exposed to a binary mixture of methane with carbon dioxide,
474 we showed that, when taking into account this second coupling, predicted
475 amounts of adsorbed fluids depend on the [loading path to which the repre-](#)
476 [sentative volume element](#) is submitted.

477 Deriving the state equations (35)-(38) in a thermodynamically consistent
478 manner and making sure that those equations could be fully calibrated was
479 a first step toward an implementation in a finite-element code and the nu-
480 merical modeling of a full CO₂-Enhanced Coal Bed Methane (CO₂-ECBM)
481 recovery process.

482 **References**

- 483 [1] N. Berkowitz, The chemistry of coal., Elsevier Science 86 (1985).
- 484 [2] J. R. Levine, Coalification: The evolution of coal as source rock and
485 reservoir rock for oil and gas, Law, B., Rice, D. (Eds.), Hydrocarbons
486 from Coal (1993) 39–77.
- 487 [3] T. Gentzis, Subsurface sequestration of carbon dioxide - an overview
488 from an alberta (canada) perspective, International Journal of Coal
489 Geology 43 (2000) 287–305.
- 490 [4] C. M. White, D. H. Smith, K. L. Jones, A. L. Goodman, S. A. Jikich,
491 R. B. LaCount, S. B. DuBose, E. Ozdemir, B. I. Morsi, K. T. Schroeder,
492 Sequestration of carbon dioxide in coal with enhanced coalbed methane
493 recovery: A review, Energy and Fuels 19 (2005) 659–724.
- 494 [5] M. Mazzotti, R. Pini, G. Storti, Enhanced coalbed methane recovery,
495 The Journal of Supercritical Fluids 47 (2009) 619–627.

- 496 [6] S. E. Laubach, R. A. Marrett, J. E. Olson, A. R. Scott, Characteris-
497 tics and origins of coal cleat: A review, *International Journal of Coal*
498 *Geology* 35 (1998) 175–207.
- 499 [7] I. Palmer, S. R. Reeves, Modeling changes of permeability in coal seams.
500 Final Report, DOE Contract No. DE-FC26-00NT40924, Technical Re-
501 port, 2007.
- 502 [8] H. Briggs, R. Sinha, Expansion and contraction of coal caused respec-
503 tively by the sorption and discharge of gas, *Proceedings of the Royal*
504 *Society of Edinburgh* 53 (1932) 48–53.
- 505 [9] S. Hol, C. J. Spiers, Competition between adsorption-induced swelling
506 and elastic compression of coal at CO₂ pressures up to 100 MPa, *Journal*
507 *of the Mechanics and Physics of Solids* 60 (2012) 1862–1882.
- 508 [10] J. Liu, Z. Chen, D. Elsworth, H. Qu, D. Chen, Interactions of multi-
509 ple processes during CBM extraction: A critical review, *International*
510 *Journal of Coal Geology* 87 (2011) 175–189.
- 511 [11] Z. Pan, L. D. Connell, Modelling permeability for coal reservoirs: A
512 review of analytical models and testing data, *International Journal of*
513 *Coal Geology* 92 (2012) 1–44.
- 514 [12] A. Grosman, C. Ortega, Influence of elastic strains on the adsorption
515 process in porous materials: An experimental approach, *Langmuir* 25
516 (2009) 8083–8093.
- 517 [13] G. Dolino, D. Bellet, C. Faivre, Adsorption strains in porous silicon,
518 *Phys. Rev. B* 54 (1996) 17919.

- 519 [14] G. Gunther, J. Prass, O. Paris, M. Schoen, Novel insights into nanopore
520 deformation caused by capillary condensation, *Phys. Rev. Lett.* 101
521 (2008) 086104.
- 522 [15] G. Reichenauer, G. W. Scherer, Nitrogen adsorption in compliant ma-
523 terials, *Journal of Non-Crystalline Solids* 277 (2000) 162–172.
- 524 [16] G. Y. Gor, A. V. Neimark, Adsorption-induced deformation of meso-
525 porous solids, *Langmuir* 26 (2010) 13021–13027.
- 526 [17] G. Y. Gor, O. Paris, J. Prass, P. A. Russo, M. M. L. Ribeiro Carrott,
527 A. V. Neimark, Adsorption of n-pentane on mesoporous silica and ad-
528 sorbent deformation, *Langmuir* 29 (2013) 8601–8.
- 529 [18] F.-X. Coudert, M. Jeffroy, A. H. Fuchs, A. Boutin, C. Mellot-Draznieks,
530 Thermodynamics of guest-induced structural transitions in hybrid
531 organic-inorganic frameworks, *Journal of the American Chemical So-*
532 *ciety* 130 (2008) 14294–302.
- 533 [19] A. V. Neimark, F.-X. Coudert, A. Boutin, A. H. Fuchs, Stress-based
534 model for the breathing of metal-organic frameworks, *The Journal of*
535 *Physical Chemistry Letters* 1 (2010) 445–449.
- 536 [20] P. I. Ravikovitch, A. V. Neimark, Density functional theory model of
537 adsorption deformation, *Langmuir* 22 (2006) 10864–8.
- 538 [21] P. Kowalczyk, A. Ciach, A. V. Neimark, Adsorption-induced deforma-
539 tion of microporous carbons: pore size distribution effect, *Langmuir* 24
540 (2008) 6603–8.

- 541 [22] G. Pijaudier-Cabot, R. Vermorel, C. Miqueu, B. Mendiboure, Revisit-
542 ing poromechanics in the context of microporous materials, *Comptes*
543 *Rendus Mécanique* 339 (2011) 770–778.
- 544 [23] L. Brochard, M. Vandamme, R. J.-M. Pellenq, Poromechanics of micro-
545 porous media, *Journal of the Mechanics and Physics of Solids* 60 (2012)
546 606–622.
- 547 [24] A. Grosman, C. Ortega, Influence of elastic deformation of porous ma-
548 terials in adsorption-desorption process: A thermodynamic approach,
549 *Phys. Rev. B* 78 (2008) 085433.
- 550 [25] F.-X. Coudert, The osmotic framework adsorbed solution theory: pre-
551 dicting mixture coadsorption in flexible nanoporous materials, *Physical*
552 *Chemistry Chemical Physics* 12 (2010) 10904–13.
- 553 [26] I. Gray, *Reservoir Engineering in Coal Seams: Part 1-The Physical*
554 *Process of Gas Storage and Movement in Coal Seams*, *SPE Reservoir*
555 *Engineering* 2 (1987).
- 556 [27] J. Seidle, L. Huitt, Experimental measurement of coal matrix shrinkage
557 due to gas desorption and implications for cleat permeability increases,
558 *International Meeting on Petroleum Engineering*. Society of Petroleum
559 Engineers, Inc., Beijing, China. (1995).
- 560 [28] I. Palmer, J. Mansoori, How permeability depends on stress and pore
561 pressure in coalbeds: a new model, *SPE Reservoir Evaluation and En-*
562 *gineering* (1998) 539–544.

- 563 [29] X. Cui, R. M. Bustin, Volumetric strain associated with methane des-
564 orption and its impact on coalbed gas production from deep coal seams,
565 AAPG Bulletin 89 (2005) 1181–1202.
- 566 [30] E. Robertson, R. Christiansen, A permeability model for coal and other
567 fractured, sorptive-elastic media, SPE Journal 13 (2008) 314–424.
- 568 [31] L. D. Connell, M. Lu, Z. Pan, An analytical coal permeability model
569 for tri-axial strain and stress conditions, International Journal of Coal
570 Geology 84 (2010) 103–114.
- 571 [32] S. Harpalani, G. Chen, Estimation of changes in fracture porosity of
572 coal with gas emission, Fuel 74 (1995) 1491–1498.
- 573 [33] J. Q. Shi, S. Durucan, Drawdown induced changes in permeability of
574 coalbeds: A new interpretation of the reservoir response to primary
575 recovery, Transport in Porous Media 56 (2004) 1–16.
- 576 [34] H.-H. Liu, J. Rutqvist, A new coal-permeability model: Internal swelling
577 stress and fracturematrix interaction, Transport in Porous Media 82
578 (2010) 157–171.
- 579 [35] J. Liu, J. Wang, Z. Chen, S. Wang, D. Elsworth, Y. Jiang, Impact of
580 transition from local swelling to macro swelling on the evolution of coal
581 permeability, International Journal of Coal Geology 88 (2011) 31–40.
- 582 [36] Y. Wu, J. Liu, Z. Chen, D. Elsworth, D. Pone, A dual poroelastic model
583 for CO₂-enhanced coalbed methane recovery, International Journal of
584 Coal Geology 86 (2011) 177–189.

- 585 [37] S. Hol, C. J. Peach, C. J. Spiers, Applied stress reduces the CO₂ sorption
586 capacity of coal, *International Journal of Coal Geology* 85 (2011) 128–
587 142.
- 588 [38] Y. Wu, J. Liu, D. Elsworth, Z. Chen, L. Connell, Z. Pan, Dual poroe-
589 lastic response of a coal seam to CO₂ injection, *International Journal of*
590 *Greenhouse Gas Control* 4 (2010) 668–678.
- 591 [39] L. Perrier, G. Pijaudier-Cabot, D. Grégoire, Poromechanics of
592 adsorption-induced swelling in microporous materials: a new porome-
593 chanical model taking into account strain effects on adsorption, *Contin-*
594 *uum Mechanics and Thermodynamics* (2014).
- 595 [40] J. Rouquerol, F. Rouquerol, P. Llewellyn, G. Maurin, K. S. Sing, Ad-
596 sorption by powders and porous solids: principles, methodology and
597 applications, Academic Press, 2013.
- 598 [41] O. Coussy, *Poromechanics*, John Wiley & Sons, Ltd, 2004.
- 599 [42] O. Coussy, *Mechanics and Physics of Porous Solids*, John Wiley & Sons,
600 Ltd, 2010.
- 601 [43] S. Nikoosokhan, L. Brochard, M. Vandamme, P. Dangla, R. J.-M. Pel-
602 lenq, B. Lecampion, T. Fen-Chong, CO₂ storage in coal seams: Coupling
603 Surface Adsorption and Strain. In: *Geomechanical issues in CO₂ stor-*
604 *age*. Ed: G. Pijaudier-Cabot, J.-M. Pereira, Wiley, pp. 115–129.
- 605 [44] S. Nikoosokhan, M. Vandamme, P. Dangla, A poromechanical model for
606 coal seams injected with carbon dioxide: from an isotherm of adsorption

- 607 to a swelling of the reservoir, *Oil & Gas Science and Technology - Rev.*
608 *IFP Energies nouvelles* 67 (2012) 777–786.
- 609 [45] L. Brochard, M. Vandamme, R. J.-M. Pellenq, T. Fen-Chong,
610 Adsorption-induced deformation of microporous materials: coal swelling
611 induced by CO₂-CH₄ competitive adsorption, *Langmuir* 28 (2012) 2659–
612 2670.
- 613 [46] D. N. Espinoza, M. Vandamme, P. Dangla, J.-M. Pereira, S. Vidal-
614 Gilbert, A transverse isotropic model for microporous solids: Appli-
615 cation to coal matrix adsorption and swelling, *Journal of Geophysical*
616 *Research: Solid Earth* 118 (2013) 6113–6123.
- 617 [47] R. Pini, S. Ottiger, L. Burlini, G. Storti, M. Mazzotti, Role of adsorp-
618 tion and swelling on the dynamics of gas injection in coal, *Journal of*
619 *Geophysical Research* 114 (2009) B04203.
- 620 [48] Z. Yangsheng, H. Yaoqing, W. Jingping, Y. Dong, The experimen-
621 tal approach to effective stress law of coal mass by effect of methane,
622 *Transport in Porous Media* 53 (2003) 235–244.
- 623 [49] Z. Pan, L. D. Connell, M. Camilleri, Laboratory characterisation of
624 coal reservoir permeability for primary and enhanced coalbed methane
625 recovery, *International Journal of Coal Geology* 82 (2010) 252–261.
- 626 [50] Z. Chen, Z. Pan, J. Liu, L. D. Connell, D. Elsworth, Effect of the
627 effective stress coefficient and sorption-induced strain on the evolution
628 of coal permeability: Experimental observations, *International Journal*
629 *of Greenhouse Gas Control* 5 (2011) 1284–1293.

- 630 [51] R. Pini, Enhanced Coal Bed Methane Recovery Finalized to Carbon
631 Dioxide Storage, Ph.D. thesis, ETH Zürich, 2009.
- 632 [52] X. Cui, R. Bustin, Volumetric strain associated with methane desorption
633 and its impact on coalbed gas production from deep coal seams, AAPG
634 Bulletin 89 (2005) 1181–1202.
- 635 [53] W. Brace, J. Walsh, W. Frangos, Permeability of granite under high
636 pressure, Journal of Geophysical Research 73 (1968) 2225–2236.
- 637 [54] R. Pini, S. Ottiger, L. Burlini, G. Storti, M. Mazzotti, Sorption of car-
638 bon dioxide, methane and nitrogen in dry coals at high pressure and
639 moderate temperature, International Journal of Greenhouse Gas Con-
640 trol 4 (2010) 90–101.